Evaporation of Water in an Aqueous Lithium Bromide Solution flowing over a Horizontal Tube

Dongkwan Kim* and Moohwan Kim**

Key words: Falling film, Film Reynolds number, Wall superheat, Knurled tube

Abstract

Falling film heat transfer analyses with aqueous lithium bromide solution were performed to investigate the transfer characteristics of the copper tubes. Finned (knurled) tube and a smooth tube were selected as test specimens. Averaged generation fluxes of water and the heat flux were obtained. As the film flow rate of the solution increased, the generation fluxes of water decreased for both tubes due to the fact that the heat transfer resistance increased with the film thickness. The effect of the enlarged surface area at the knurled tube was supposed to be dominant at a small flow rate. The generation fluxes of water increased with the increasing degree of tube wall superheat. Nucleate boiling is supposed to occur at a wall superheat of 20 K for a smooth tube, and at 10 K for a knurled tube. The increased performance of the knurled tube was supposed to mainly come from the effect of the increased heating surface area.

Nomenclature

A : heat transfer area [m^2]
C_p : specific heat of the solution [J/kg-K]
h_f : film heat transfer coefficient [W/m^2K]
H : heat of absorption [J/kg]
$\dot{m}$: mass flow rate [kg/s]
m'' : evaporation flux [kg/m^2-s]
P : system pressure [Torr]
q'' : heat flux [W/m^2]
q''_e : evaporative heat flux [W/m^2]
q''_s : sensible heat flux [W/m^2]
Re_f : film Reynolds number [$4\Gamma/\mu$]
T : temperature [℃]
T_{sat} : degree of wall superheat [℃]
w : LiBr concentration [wt%]
Γ : mass flow rate per unit length [kg/m-s]
μ : viscosity of the solution [kg/m-s]

Subscripts

sat : saturation
sol : solution

* System Engineering Division, Institute of Advanced Material Study, Kyushu University 6-1, Kasuga-kohen, Kasuga 816-8580, Japan
** Department of Mechanical Engineering, Pohang University of Science and Technology San 31, Hyoja-Dong, Nam-Gu, Pohang, Kyungbuk 790-784, Korea

w : wall

1. Introduction

The absorption heat pump system is considered to be a good replacement for the vapor compression type refrigeration with the merits on costs and environmental aspects.[1] Particularly, in a system using aqueous lithium bromide solution as a working fluid, low grade energy such as waste heat can be used as a heat source for the generator. On a standard cycle, the evaporator and the absorber are operated at a low temperature and pressure, but the generator and the condenser are operated at a high temperature and pressure. In fact, heat and mass transfer with the phase change occurs simultaneously in the absorber and the generator. The absorption and generation processes are chiefly governed by the heat and the mass transfer with the mass diffusion. Hence, the heat and mass transfer processes on these systems are complex, and the analyses of these phenomena are important for the system compactness and performance increment.

Previously, the generator was of a pool boiling type because it used high grade energy such as oil or gas for a heat source.[2-4] But nowadays, the falling film type of heat exchanger for steam generation is known for its good applicability when it uses low grade energy such as waste heat for a heat source.[5] These phenomena in turn must be analyzed with the heat and mass transfer processes because the evaporation process on the falling film surface changes the solute (LiBr) concentration drastically.

When the liquid film flows down the outside of a heated horizontal tube, water in a mixture evaporates by the temperature difference between the tube wall and the liquid film. For this case, LiBr concentration drastically changes by the evaporation of water and this process accompanies the mass transfer by the concentration difference inside the liquid film.

This report shows the experimental results on falling film heat transfer flowing over a horizontal tube. Two kinds of copper tubes were used. The solution flow rate and the wall superheat were varied as test parameters.

2. Experiment

Figure 1 shows the schematic diagram of the experimental apparatus. The system was constructed with four flow paths. The solution line has two feed tanks, a solution pump, an auxilliary heater and a generator (test section). The heat source line has a constant temperature bath and a hot water pump to circulate the hot water as a heat source to the inside of the horizontally arranged test tube. The steam line was constructed to measure the amount of generated steam. It has a steam duct and a condensate collector. The generated steam at the test section flowed out through this steam line and was condensed at the condenser to measure the weight of the condensed water. The coolant line was also constructed to condense the steam in the steam line, and it has a condenser, a cooling water pump and a constant temperature bath.

For our experiment, smooth copper tube and the knurled tube arranged horizontally at the test section were used (Table 1). At a feed

Table 1 Specification of the test section

Tube name	Dimensions (mm)	Ratio of surface area based on smooth tube
Smooth	Outer diameter=19.05 Thickness=1.07	1
Knurled 	Outer diameter=19.05 Thickness=1.09 26 fins/inch Fin pitch=0.7 Fin height=0.45	3

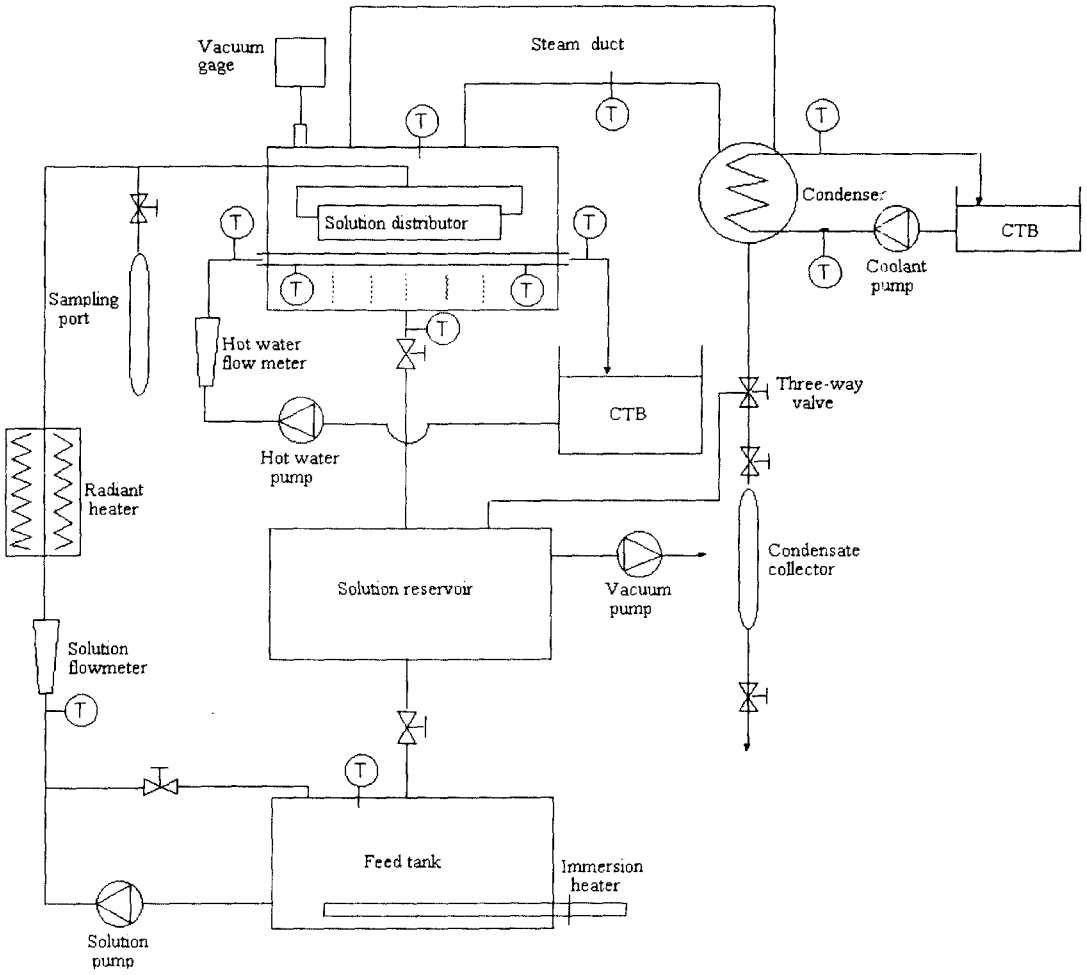

Fig. 1 Schematic diagram of experimental apparatus.

tank, aqueous LiBr solution was heated to a saturation temperature on the bases of operating pressure and LiBr concentration by the electric immersion heater. The magnetic solution pump sent it to the test section through the volumetric flow meter and the auxiliary radiant heater. Hot water, as a heat source, was circulated in the inside of the horizontally arranged test tube. At the test section aqueous LiBr solution was circulated along the outer surface of the horizontally heated tube through the solution distributer and then returned to the feed tank. At the inlet of the test section, a sampling port was used to sample out the solution in order to determine the LiBr concentration with the density meter. The LiBr concentration was used as a test parameter. To measure the pressure at the test section, an absolute vacuum gage was set up. For these experiments, a solution distributer was positioned 11 mm above the heated tube, and the distributing system was a plate type perforated with 2 mm holes and the hole pitch was 4.5 mm. The amount of generated steam was measured with a condensate collector after condensing the steam with a condenser at a steady state.

The film Reynolds number and the degree of

Table 2 Experimental conditions

Parameter	Value
LiBr concentration (wt%)	53
System pressure (Torr)	60
Wall superheat (K)	2.5~30
Film Reynolds number	50~500

wall superheat are defined as follows:

$$\mathrm{Re}_f = 4\Gamma/\mu \quad (1)$$

$$\Delta T_{sat} = T_w - T_{sat} \quad (2)$$

The experimental conditions are shown in Table 2. The flow regime is wavy-laminar in the falling film, and the moderate film Reynolds number was set up with the flow valve. To measure the average tube wall temperature T_w, T-type thermocouples with an accuracy of 0.1 ℃ were seamed on the tube surface with 8 points at each end of the tube. Thermocouple grooves around the circumference were 1 mm wide and 0.5 mm deep. A highly conductive epoxy was used to bond it. To compensate for the temperature error from thermocouple wire, the thermocouple wires were calibrated after it was assembled. The averaged value of the tube wall temperatures measured at 8 points was taken as the mean wall temperature. Heat flux through the tube wall was defined as follows;

$$q'' = q''_e + q''_s = m'\Delta H + mC_p\Delta T_{sol}/A \quad (3)$$

Thus, the transfer performance on film evaporation at a steady state was analysed with each parameter.

3. Result and discussion

3.1 Effect of the solution flow rate

Figure 2 shows the variation of steam generation flux with the film Reynolds number defined in equation (1). The steam generation flux was decreased as the film Reynolds number increased. This was caused by the fact that the heat transfer resistance due to the film thickness was increased as the solution flow rate increased. The decrease slope in the knurled tube was larger than that of the smooth tube. The effect of fin was large at a small flow rate especially. But the effect of fin reduced as the flow rate increased. The increase ratio of steam generation flux for

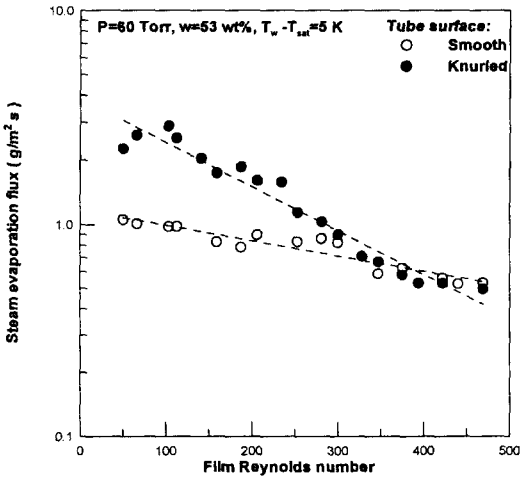

Fig. 2 Steam evaporation flux with solution flow rate.

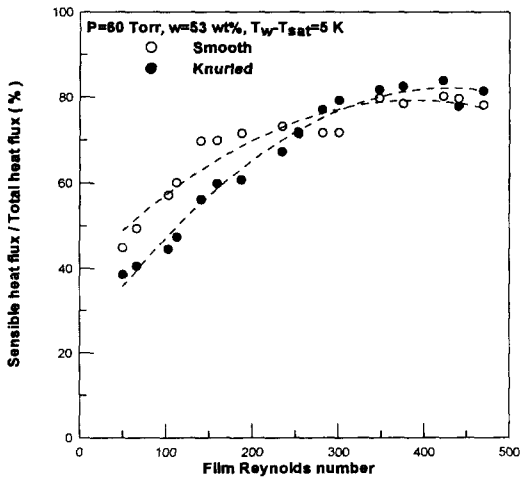

Fig. 3 Fraction of sensible heat flux with solution flow rate.

knurled tube at a small flow rate was about 3 times larger than that of the smooth tube which was the area increase ratio.

Figure 3 shows that the fraction of sensible heat flux on total heat flux, which was defined in equation (3). This fraction increased with film Reynolds number. However it was slightly decreased at the flow rates larger than $Re_f = 400$. It was shown that the effect of the fin on the knurled tube was large at small flow rate due to the increase of heat transfer area. At a small flow rate, the latent heat flux was increased by the increase of the heating surface area, and the effect was decreased as the flow rate increased by the increase of heat transfer resistance with the increase of film thickness.

3.2 Effect of wall superheat

Figure 4 shows the steam generation flux with the variation of wall superheat at a constant solution flow rate. The steam generation flux was increased as the wall superheat increased by the increase of driving temperature difference between wall and the liquid film. The evaporation performance of the knurled tube at small wall superheat shows nonlinear trend with the increase of wall superheat due to the effect of fin geometry.

Figure 5 shows the heat flux ratio with the variation of wall superheat. Sensible heat flux for a smooth tube charged about 50% to the value of 20 K on wall superheat and the ratio decreased steadily after that value. For the knurled tube, the decrease rate of the heat flux ratio shows different trend. The fraction of sensible heat flux decreased at low wall su-

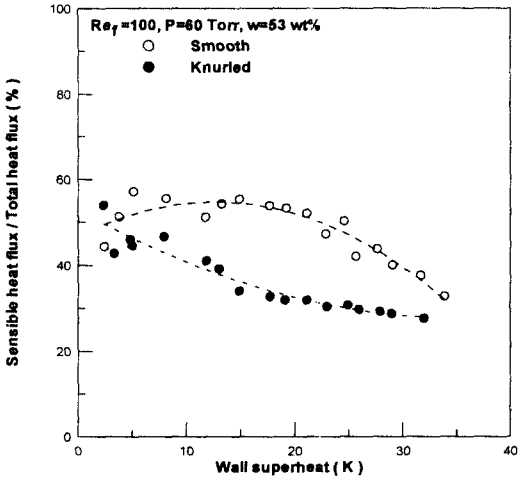

Fig. 5 Fraction of sensible heat flux with wall superheat.

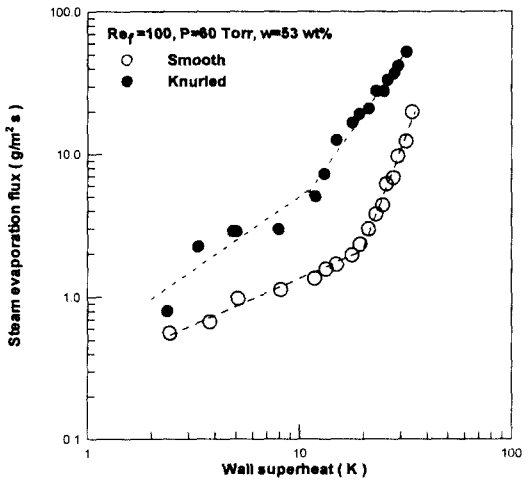

Fig. 4 Steam evaporation flux with wall superheat.

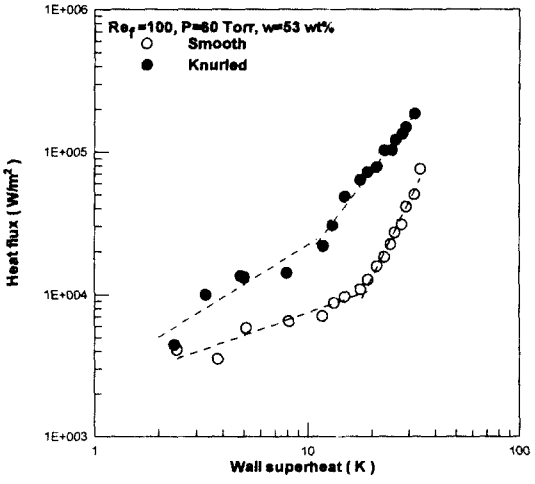

Fig. 6 Performance of total heat flux with the wall superheat.

Table 3 Uncertainties of film heat transfer coefficients

Tube surface	Smooth		Knurled	
Heat flux (W/m^2)	3537.2	75963.9	4466.7	186370
Heat transfer coefficient (W/m^2K)	1676.8	2242.7	1884.7	5836.8
Uncertainty (%)	5.63	4.57	6.52	4.57

perheat and its slope was reduced at high wall superheat. The steam generation flux at low wall superheat was not so large for the knurled tube compared with wall superheat above 10 K. However most heat flux on the knurled tube was used to generate the steam above 10 K of wall superheat.

Figure 6 shows the comparison on total heat flux with the previous pool boiling data. Nucleation was supposed to occur at a wall superheat of 20 K for the smooth tube, and at 10 K for the knurled tube. The structure of the knurled tube was thought as sufficient condition to generate the nucleate boiling.

3.3 Uncertainty analysis

For these experiments, the steady-state measuring time was approximately 5 minutes for each parameters, and the data points were plotted on graphs with a maximum deviation of 9.4% for wall superheat (Re_f: 6.8%, P: 1%, w: 0.3%). The uncertainty for film heat transfer coefficient,[6] defined in equation (4), at an ultimate case of heat flux is shown in Table 3.

$$h_f = q'' / \triangle T_{sat} \tag{4}$$

4. Conclusions

The steam generation flux and heat flux was studied with experiment on horizontal falling film. The smooth and the knurled tubes were selected as test specimens. The controlled parameters were a solution flow rate and the wall superheat. Steam generation flux decreased as the solution flow rate increased. Steam generation flux increased as the wall superheat increased. Nucleation was presumed above a certain wall superheat. Falling film heat transfer is prior to pooling at low wall superheat of 10 K for both tubes. The performance increase on heat flux and steam generation flux of the knurled tube comes from enlarged heat transfer area.

References

1. Minton, P. E., 1986, Handbook of evaporation technology, Noyes Publications, pp. 70-84.
2. Ishibash, E. and Iwasaki, K., 1982, Results of boiling experiments for solar powered absorption type chiller (report 1), Transaction of Japanese Association of Refrigeration, Vol. 57, pp. 231-238.
3. Nishimatsu, A. et al., 1979, Pool boiling heat transfer to lithium bromide water solution under vacuum, Heat Transfer Japanese Research, Vol. 8, pp. 1-15.
4. Ohnishi, M. et al., 1978, Pool boiling heat transfer to lithium bromide water solution, Heat Transfer Research, Vol. 7, pp. 67-77.
5. Fujita, T., 1993, Falling liquid films in absorption machines, International Journal of Refrigeration, Vol. 6, pp. 282-294.
6. Jong H. Kim and Terrence W. Simon, 1993, Journal of heat transfer policy on reporting uncertainties in experimental measurements and results, Journal of Heat transfer, Vol. 115, pp. 5-6.